Experiments in Fluids 12, 261–269 (1992)

Experiments in Fluids

Speed measurements in the developing region of an electrohydrodynamic spray using laser diagnostics

J. M. Grace and **P. F. Dunn**

Particle Dynamics Laboratory, Dept. of Aerospace and Mechanical Engineering, University of Notre Dame, Notre Dame, IN 46556, USA

Abstract. Experiments were conducted to assess the ability of a particle-counter-sizer velocimeter (PCSV) to measure droplet speeds in the developing region of an electrohydrodynamic spray. The working fluid, ethanol, was pumped through a stainless steel capillary tube at a constant mass flow rate. The capillary tube was held at various positive potential voltages with respect to an externally grounded funnel located below the tube. Data were acquired at two axial stations, directly under the capillary tip, in the developing region of the subject spray. The results indicated that the PCSV, with an experimental modification to the speed reduction process, performed well in this region. Speeds were measured at the near station within an average uncertainty of 2.2% and a corresponding maximum uncertainty of 3.0%; speeds at the far station were measured within an average uncertainty of 4.6% and a corresponding maximum uncertainty of 6.0%.

1 Introduction

The process of disrupting liquids into fine droplets of known size for their subsequent dispersion presents many technological advantages over the bulk distribution of a liquid. The ability to precisely regulate the generation process of the droplets allows for a greater degree of control in the particular application of the liquid, e.g., paint spraying and fuel atomization, through increased and regulated surface-to-volume ratios. Several methods for generating these types of aerosols exist. Some include pressure, ultrasonic and electrohydrodynamic (EHD) atomization. The EHD atomization technique provides an additional controlling parameter: the electric charge on the droplet. Controlling an atomization process, however, implicitly assumes that the process is physically well-understood. This presently is not the case for EHD atomization. This process, in general, can be described by the forces involved in the breakup of the liquid column that subsequently forms the droplets. The resultant interaction of these forces, however, as well as the effect of the experimental parameters on droplet formation and dispersion per se still remain elusive.

This paper does not seek to answer fundamental questions about droplet generation, but rather to define the applicability of a measuring device to a region where the fundamental laws are the most assailable. This region, referred to as the developing region, exists in the fine spray mode of the EHD spray near the capillary tip. The fine spray mode describes only one of several EHD spray modes (Drozin 1954). The developing region is defined from the needle tip to the location where spherical droplets dominate the droplet shape distribution. Examination of the developing region requires consideration of its characteristically complex geometry and sensitivity to external perturbations. This study specifically investigates the possibility of measuring droplet speeds in this region with a laser-based, single-particle counter, the particle-counter-sizer velocimeter (PCSV). In the present experiments only the capability of accurate droplet speed measurement was assessed.

The droplets in the fine spray mode are essentially formed from the breakup of relatively short ligaments, as seen in stroboscopic photography (Snarski 1988). Based on this production process, the droplets will eventually relax to the minimum energy state of a sphere. This spherical state results from the low relative velocity between the ambient air and the droplet. Droplet production from ligament collapse is governed by two time constants: one, the time required for a resulting ligament segment to collapse to a sphere, and two, the time required for the resultant oscillations from this collapse to die out. These time constants govern the extent of the developing region.

Experiments that seek to measure spray parameters in the developing region must satisfy several criteria. The most basic restriction on the measurement device requires nonintrusive sampling; a restriction that fits well into the characteristics of light-based devices. Although several light-based techniques exist, those based on light scattering from single particles perform data acquisition on this type of phenomenon best. A further restriction on the measurement device results from the definition of the developing region, i.e., that region where the initial "droplet" formed will not be spherical.

The PCSV satisfies these criteria. The PCSV technique offers the capability of nonintrusive, real-time measurement of droplet/particle size and speed in a flow field. This device

also has a distinct advantage in its ability to resolve size and speed for droplets/particles with length-to-width aspect ratios of up to 2 : 1. This ability greatly enhances the attractiveness of the technique for investigations near the generation point of an atomization process. This ability, however, can lead to erroneous measurements without proper consideration of the subject phenomena and the resulting interpretation of the measurement technique. Other measurement techniques, specifically, Doppler scattering, have been used to investigate droplet velocities in an EHD spray (Dunn and Snarski 1991, Snarski 1988). However, these techniques do not satisfy the criteria for generation region measurements and must be restricted to regions where spherical droplets dominate the shape distribution.

In the subject experiment, data are acquired at two axial measurement stations directly below the needle's tip (0.0 cm radial). Herein, measurements are restricted to the calculated extent of the developing region. Calculations (Grace 1990) show that droplets at the first measurement station certainly can exhibit the oscillatory characteristics of nonspherical droplets, while those at the second measurement station have a high probability for completely damped oscillation and a subsequent spherical shape.

This investigation assesses the ability of the PCSV to resolve droplet speeds. This information is important when considering the atomization process in terms of its kinetic energy ($m|V|^2/2$). The effect of variable aspect ratio droplets on the speed determination is also investigated. This analysis concentrates on the speed errors involved with the inclusion of "droplets" having various aspect ratios as well as those associated with the application of the technique itself. These application errors involve calibration of the equipment, variability in speed measurement as a function of user specified input (a fuzzy validation criterion) and, finally, the error associated with the speed computation algorithm itself. Further, the assumptions made in this experiment specific to the PCSV theory of operation and those made to simplify the results are discussed. This primarily concerns the effects on the PCSV's ability to measure droplet speed and the restrictions imposed on the experimental parameters as a result of these necessary operating assumptions.

2 Experimental apparatus and procedure

This section details the experimental apparatus, shown schematically in Fig. 1, and the experimental procedure. In the subject experiments, the working fluid, ethanol, is pumped at a constant mass flow rate of 5 mg/s through a 27 gauge stainless steel hypodermic needle (216 μm I.D., 406 μm O.D., 1.905 cm length) located approximately 38 cm from an electrically grounded collection funnel. The fine spray mode criteria restricts the operating potential between the capillary tube and the funnel to a range of 15 kV–27.5 kV.

The experimental apparatus can be divided into three general blocks: data generation, data acquisition, and data reduction. The first block consists of the droplet generator, the EHD spray (droplets) and the PCSV. A reticle, replacing the EHD spray, simulates droplets in the calibration procedure. The droplet generator contains the electrically isolated capillary tube, a liquid feed line, and a high-voltage connection. The EHD spray results from the application of the high-voltage potential between the capillary tube and the electrically grounded funnel. The dimensions of the capillary tube concentrate the electric field near the tip to sufficiently high levels ($\sim 10^6$ V/m) such that inherent instabilities in the flow are magnified to the point of droplet production (Bailey 1988; Snarski 1988). The violent instabilities of the liquid, coupled with the now important aerodynamic shear force, act in tandem with the electric forces (Coulombic and external field) to disperse the droplets, thereby resulting in an EHD aerosol.

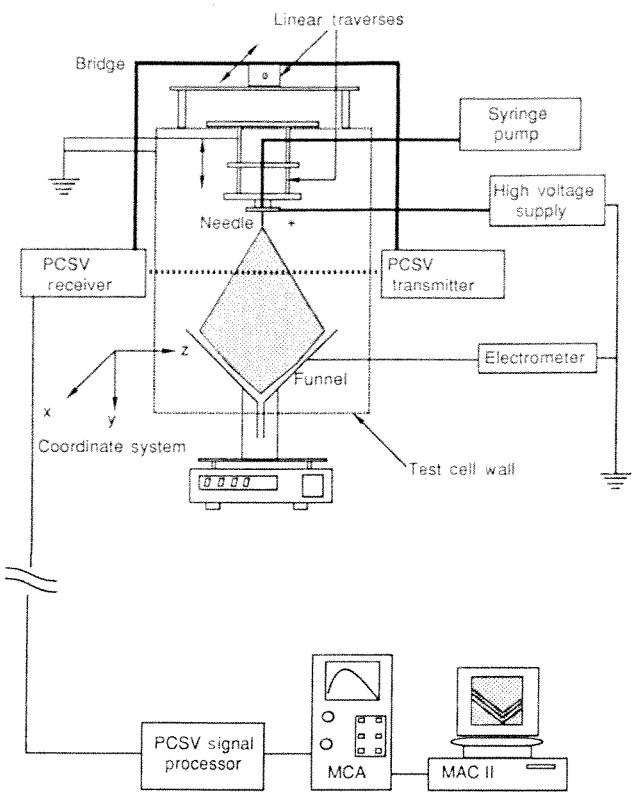

Fig. 1. Experimental schematic

An Insitec RS-2 reticle (Insitec, San Ramon, Calif.) simulates the droplets for speed calibration. This device basically consists of an opaque disk with holes of known size etched through it at known locations. The disk is surrounded by lens quality glass and connected by a belt to a DC motor such that it rotates the holes through the measurement volume. This rotation simulates droplet trajectories (motion). The design of the reticle allows for size and speed calibration. It also has the capability of determining the measurement volume intensity distribution in all directions.

The final component of the data generation block is the PCSV system. The present experiment uses the system only

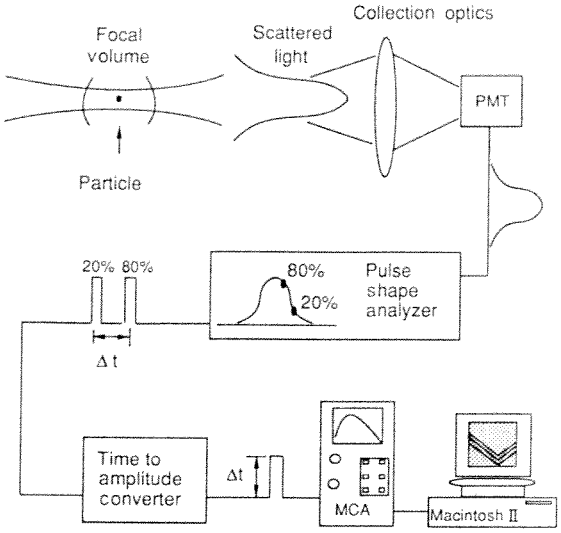

Fig. 2. Droplet signal processing path

to generate raw data. The data reduction utilizes the PCSV speed measurement theory, but it is performed independently of the PCSV software reduction package. Hence, only the PCSV hardware and controlling software are of interest here. This experiment uses an Insitec PCSV model PCSV-E (1985) which is configured to record 4°, off-axis, forward-scattered light in the diffraction-dominated regime. A single, focused 5 mW HeNe laser ($\lambda = 0.632$ μm) generates the measurement volume. The PCSV-E is controlled by Insitec PCSV software, Dual Beam Version (1987). See Insitec (1990) for general information on the PCSV-E. The droplet diameter range applicable to this experiment is from ~3 μm to ~50 μm. The light scattered by a droplet traversing the measurement volume is converted to an electric signal by a photomultiplier tube, as shown in Fig. 2. This signal is then sent to a pulse shape analyzer (PSA) circuit which discriminates out signals below a selected voltage and generates an output pulse at each of the 20% and 80% fractional amplitudes of the signal peak amplitude. These pulses are sent to a time-to-amplitude converter (TAC) which discriminates out signals greater than a selected width. The TAC generates a pulse with a height proportional to the time difference between the fractional amplitudes. This signal is then sent to the PCSV-E reduction software. The specifics on the PCSV-E theory of operation are discussed in Section 3.

Data acquisition and data reduction are performed sequentially by a multi-channel analyzer (MCA) and a Macintosh II personal computer (Apple, Cupertino, Calif.). The PCSV-E raw data, i.e., the TAC signal, is acquired on the MCA. This distribution is then downloaded to the Macintosh II, where it is manipulated as detailed in the procedure.

The experimental procedure follows in the same three blocks as those of the experimental apparatus. The experiments are conducted at six applied voltages from 15 kV to 27.5 kV and acquired at two axial stations along the spray centerline. The method for acquisition treats each measurement location separately. The data is acquired in series from low to high applied voltage and repeated such that at least five measurements determine the final average speed for a given set of parameters. Data are acquired over several days, with prolonged delay time, to ensure repeatability.

The data reduction procedure involves manipulating the MCA data through experimentally determined conversion factors, and calculating a weighted average of the resulting speed distribution. The weighted average technique follows from standard statistics and generates a representative number for the speed distribution used in the presentation of results. The cutoff voltages (Section 4) used in the final presentation are experimentally determined by examining at least 400 samples per voltage per station. The samples are acquired on an oscilloscope, identified as one of five possible types and catalogued.

The calibration procedure generates data by rotating the reticle through the measurement volume. The data is acquired and reduced in three ways in order to cross-check experimental constants. Various combinations of data acquisition and reduction lead to three distinct approaches to determine the reticle speed. These are: (1) measuring the period of rotation and using the known radius of the reticle particles, (2) using the complete PCSV-E system (including reduction software) and (3) recording the output of the PCSV-E hardware (TAC) on the MCA, calculating a weighted average and dividing the PCSV-E referenced transit time distance by this average transit time.

3 Specifics of operation and reduction

This section outlines the basic principles of the PCSV-E speed measurements and also discusses the presentation of errors in terms of confidence levels.

3.1 PCSV-E operation

The ability of this measurement system to measure non-spherical particles is critical to this type of experiment. The source of this unique feature lies in the formation of the measurement volume. Unlike Doppler-based systems, this technique uses a single, focused laser beam in the measurement volume and therefore does not create interference fringes. The lack of fringes allows the measurement volume to have an isotropic scattering response (Innes and Bloom 1966; Wilson and Hawkes 1987). Hence, droplets with identical deviations from the spherical case, but with different orientations and trajectories in the measurement volume, will result in identical scattering signals. The deviation in the scattered signal from the ideal case is insignificant for droplets with aspect ratios of up to 2 : 1. Because the scattering from a droplet of this type is defined not just for one orientation and trajectory but for all orientations and trajec-

tories in the measurement volume, this deviation can be accepted as valid.

Speed measurements inherently rely on the similarity and uniqueness of the Gaussian distribution (Holve and Annen 1984). The speed of a droplet traversing any path can be found by measuring the time difference between any two constant-intensity fractions of a scattered signal, i.e., the transit time, and dividing an analytical distance (TTD), specific to these constants, by this time difference. The distance and the time are properties of the similarity and the uniqueness of the Gaussian distribution, respectively. The intensity distribution in the x-y plane, $I(r)$, is governed by the Gaussian intensity distribution function (Innes and Bloom 1966; Holve and Self 1979):

$$I(r) = I_0 \exp\left(\frac{-2\,I^2}{w^2}\right). \tag{1}$$

Here, r, I_0 and w are the radial coordinate, the intensity at the focal point and the radius of the beam, respectively. As a result of the Gaussian distribution in the x-y plane, any diameter of this plane (circle) will have a Gaussian distribution. By similarity, any linear cut in this plane will result in a Gaussian distribution with a peak amplitude located on the diameter perpendicular to the cut. Similarity also allows any cut to be referenced to the diameter parallel to the cut. Because the diameters all exhibit identical Gaussian curves, the distance between two fractional intensities for any such curve, the TTD, will be the same for any diameter. Therefore, if similarity allows the reference of any cut to its parallel diameter as a transform constant, then using this constant, the distance between the fractional intensities of the diameter and the time between the fractional intensities of the cut, the droplet speed can be determined.

It is important to note that the speed measurement theory utilizes three key assumptions in speed determination to ensure the beam acts as a linear operator. They are: one, that only one droplet is in the measurement volume at a time; two, that the droplet crosses the measurement volume with a constant speed; and three, that the droplet has a linear trajectory perpendicular to the axis of transmission (i.e., in the x-y plane) while traversing the measurement volume. Violations of these initial assumptions can generate unacceptable errors and invalidate the process. The previously discussed experimental range of droplet sizes can also be included as an assumption to retain the linear operator character of the beam. An additional assumption not related to the linear operator character of the beam, but concerning a more intuitive aspect of the speed theory, involves the beam diameter and, consequently, the TTD. This parameter is assumed constant along the length of the measurement volume.

Speed theory states that the distance between any two constant intensity fractions (I/I_0) is a unique function of the beam diameter (Hirleman 1978). This can be shown using Eq. 1. Substituting into Eq. 1 an expression of the symmetry of the x-y plane ($r^2 = x^2 + y^2$), making use of the constant speed ($|V|$) assumption where $y = |V|\,t$, recalling that the maximum intensity for any cut will be on its perpendicular diameter and can therefore be expressed by Eq. 1, yields Eq. 2:

$$\frac{I(x, y)}{I(x, 0)} = \exp\left(\frac{-2\,|V|^2\,t^2}{w^2}\right). \tag{2}$$

The left-hand side of Eq. 2 is essentially the fractional intensity for the y-position of a given cut. Specifying this value as a constant and taking the difference between two such constants yields a unique time difference, the transit time, which is a function only of the droplet speed. The TTD, used in conjunction with this time to determine droplet speed, results from the resubstitution of $|V|\,t = y$ in the right-hand side of Eq. 2 and then solving for the difference in the y-position between the two specified, fractional intensities.

The PCSV-E executes the speed measurement by dividing the above analytical distance (TTD) by the time difference measured through the PSA-TAC combination. Note that the lack of orientation of the measurement volume results in identical measurements for any arbitrary direction. Hence, the PCSV-E measures speed and not velocity.

Justification of the above speed measurement assumptions and the restrictions imposed on the subject experiment due to their implementation follow. Satisfaction of the first assumption relies on the distribution and number density of the subject aerosol. Assuming the EHD spray follows a typical aerosol distribution, the droplets are randomly distributed, globally, throughout the spray. Whether or not multiple droplets are in the measurement volume at a given time depends on the number density of the flow versus the size of the measurement volume. The dimensions of the PCSV-E measurement volume allow for valid number concentrations of up to 10^6/cc. Typical concentrations seen in the subject EHD spray are of the order of 10^2–10^4/cc. Hence, on a statistical basis, the first assumption is valid.

The second assumption concerns the possibility of an accelerating droplet. The results of the present experiment show that the droplets are certainly decelerating in the developing region. However, the question is whether or not they are decelerating within the measurement volume. Considering the dimension of the measurement volume, a 10% change in speed requires a force of 80 nN on a 20 μm droplet. Calculations (Grace 1990) on a 20 μm droplet of the forces present in the spray (gravitational, Coulombic repulsion, drag and external electric field) show that the forces can at most effect a change of less than 4% in the droplet speed during transit through the measurement volume. This change in speed does not result in a significant deviation from the linear operator character of the beam. Hence, the second assumption is valid.

The third assumption has two parts: one, a linear trajectory and two, a path in the x-y plane. The above argument for insignificant acceleration in the measurement volume also satisfies the linear trajectory assumption. The effects of droplets traversing paths not in the x-y plane is the subject

of future work and can only be discussed generally. The analysis requires knowledge of the signal shape dependence on droplet trajectory. This dependence can then be used to determine a correction factor to the TTD, such that the new TTD reflects the increased path length of the droplet. The present experiment restricts data acquisition to along the spray centerline, thereby taking advantage of the spray symmetry to minimize the effects of droplet trajectories. Errors from droplets traversing the measurement volume out of the x-y plane are summarily neglected.

Because the measurement volume is formed by a focused laser beam, the assumption concerning a constant beam diameter is obviously not true. However, the variation in beam diameter with the z-direction is a function of the discrimination level to which the speed measurements are effectively restricted. It has been shown that the beam diameter of a single focused laser beam through diffraction-limited optics does not vary significantly for high discrimination levels (Hirleman and Stevenson 1978). The PCSV-E incorporates this concept in the speed measurements by restricting measurements to the 1/e intensity level from the standard definition for beam extent of $1/e^2$ intensity level. The beam diameter variation for the 1/e intensity level is less than 1% for approximately 75% of the measurement volume length, and is within 3% agreement over the entire measurement volume length. Errors from the variation in beam diameter are, therefore, neglected.

3.2 *Experimental confidence level*

The errors calculated in this experiment describe the accuracy of the speed measurements. According to the definition of the uncertainty (Abernathy et al. 1985), which results from a combination of the random and systematic or bias error components, accuracy can only be valid when compared to an acceptable standard. The experiment lacks an acceptable calibration standard, and, as a result, must express a conditional confidence level for the measurement accuracy. This level is calculated to be 57%.

In general, data presentation follows the format of $x = \underline{x} \pm n\,\sigma$ with φ % confidence (Kline 1985). Here x represents a parameter to be repeatedly measured, i.e., speed, time or distance, $\underline{x}$ the resulting average, σ the standard deviation, n a value chosen to indicate the extent of data coverage by the error limits ($\pm n\,\sigma$) and φ the confidence with which the average represents the true or accepted value of the measured quantity. If an acceptable comparison standard does not exist, as in this experiment, experimental precision can be determined, but not experimental accuracy, as defined by Kline (1985). Therefore, the confidence level can, at best, be used to describe the probability that $\underline{x} = x$ (true). As stated above, the results of this experiment are presented as accurate with a conditional confidence level defining the probability that an unknown bias error does not exist. The remainder of this section deals with the derivation of this confidence level.

The procedure used to measure the experimental speed (Sec. 4) is an exact analogy to one of the calibration speed techniques. Hence, errors associated with the calibration sequence apply directly to the actual experimental data and the problem of quantifying the bias error can be effected using the calibration data. The calibration data, resulting from three independent speed measurement techniques, show each technique with a high precision and that all three agree to within the experimental uncertainty. Two of the techniques, herein referred to as (1) and (2), measure the same physical quantities, distance and time, similarly referred to as (D) and (t), respectively. Combining these measured quantities can restrict the influence of the bias error.

Assuming that the bias errors for independent techniques are themselves independent, and defining the four possible speed measurement combinations as $sp[1] = D(t)/t(1)$, $sp[2] = D(2)/t(2)$, $sp[3] = D(2)/t(1)$ and $sp[4] = D(1)/t(2)$, yields the following results. If sp[3] and sp[4] agree (all agreements are assumed to be within experimental accuracy), then the bias error follows one of three cases: (a), it is either in (1) and (2) as well as in (D) and (t), but equivalent through the ratio $D(i)/t(j)$; (b), it is in (1) and (2) and not in (D) and (t); or (c), the bias error does not exist. If sp[1] and sp[3] agree and sp[2] and sp[3] also agree, then the bias error in $t(1)$ equals that in $t(2)$ and the same can be said for D(1) and D(2). Given that all these agreements exist in the calibration data, the later agreements (sp[1, 3] and sp[2, 3]) eliminate case (a). Therefore, the bias error either does not exist or it is equal for each technique.

The third technique measures a time and a fundamentally different physical distance, both of which are several orders of magnitude greater than the previous quantities. This technique can be described by $sp[5] = D(3)/t(3)$. Because the time measurement differs from the previous techniques only in magnitude, its bias error is assumed to behave proportionally. However, the distance measurement has no relation to the previous methods and, therefore, cannot be assumed to behave in any similar fashion. If sp[5] agrees with sp[1, 2, 3], as shown through the calibration data, then the bias error in D(3) must behave proportionally with that of D(1, 2). These conclusions imply that the speed measurements for three independent techniques either (a), have no bias error or (b), have identical bias errors.

The above analysis establishes only that the bias error is either zero or identical for all three techniques. It says nothing about an associated confidence level concerning the accuracy of the speed results. A further assessment of the bias error can be made by considering the probability that three independent measurement techniques, each with an associated independent bias error, can have identical bias errors. The basis for this rests on the assumption that the bias errors are dependent on the measurement technique and that the bias errors in N techniques will form a random set. In any random set, the probability of selecting N identical values from the set decreases with increasing N. Thus, the probability that N techniques, each having a randomly

associated bias error, will give the same result can be ascertained.

In applying this approach to the present experiment, the composite average of 210 samples, consisting of 70 samples for each technique, was computed to determine the maximum deviation between this composite average and the average of any one technique. This average-difference value was normalized by the standard deviation of the 210 samples and used as the z value in the normal distribution function ($\sim e^{-z/2}$) to determine the area under the normal distribution curve and, hence, the probability that the averages agree to within the calculated difference.

This method implicitly assumes that the composite average equals the average of a very large population. Using a random number generator to simulate a normal distribution and calculating averages in a direct analogy to the calibration data and procedure, yields a 68% probability that the composite average will represent the true population average, to within $\pm 10\%$.

Now considering the z value calculated above and referring to probability tables for a normal distribution, there is a 15.8% chance that the three techniques will indeed agree to within the calculated limits. 100% minus the probability of agreement is equivalently the probability that a bias error does not exist. Because this result is predicated on the assumption that the composite average represents the population average, the experimental confidence level results from the combination of these two uncertainties as dependent events. Hence, the experimental confidence level is calculated to be 57%.

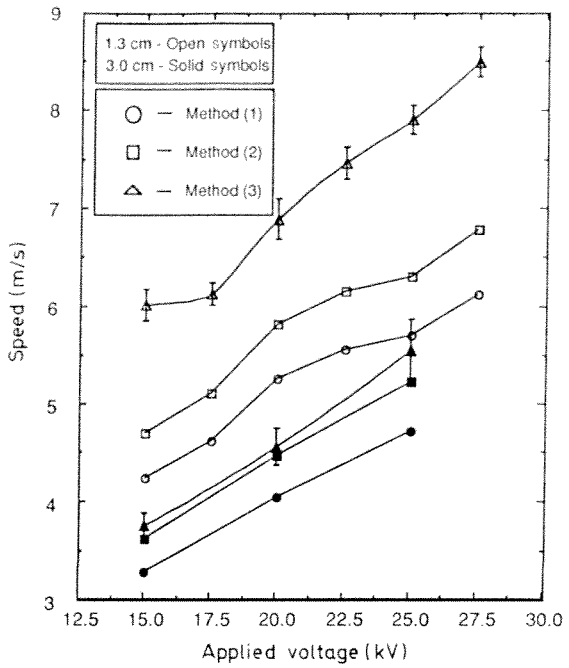

Fig. 3. Experimental speed results

4 Results and discussions

The experimental speed results are presented in Fig. 3. This figure presents and compares the three methods of speed determination. These methods are: (1) the speed determined using the weighted average of the complete MCA profile and the PCSV-E referenced TTD; (2) the speed determined using the weighted average of the complete MCA profile and the experimentally calibrated TTD; and (3) the speed determined using the weighted average of the MCA profile modified by the cutoff voltage method and the calibrated TTD. The data in Fig. 3 includes all three methods at both axial measurement stations for all the applied voltages investigated. The speed difference between methods (1) and (2) results from the calibration procedure, whereas the speed difference between methods (2) and (3) results from the characteristics of the EHD spray, which determine the cutoff voltages. These differences are discussed in more detail later in this section. Note that the data exhibits the general trends of increasing speed with increasing applied voltage and decreasing speed with increasing distance from the generation point, as seen by several investigators (Snarski 1988; Hayati et al. 1987; Gomez and Tang 1990). The error bars shown for method (3) in Fig. 3 are of primary consideration here. They show that the PCSV-E has the ability to measure droplet speed to within an average uncertainty of 2.2% (minimum 1.8% and maximum 3.0%) at the 1.3 cm measurement station and to within an average uncertainty of 4.6% (minimum 3.7% and maximum 6.0%) at the 3.0 cm measurement station.

4.1 Experimental method: cutoff voltages

Next, the results from the data reduction process followed up by an error analysis of the measurement technique are discussed. Measuring the speed of droplets in the developing region requires consideration of the nonspherical nature of the droplets. Although the PCSV-E technique has the ability to measure droplets with aspect ratios of up to 2 : 1, the existence of droplets with aspect ratios greater than 2 : 1 cannot be discounted. Therefore, additional analysis is required to account for their presence.

In this experiment, a variety of characteristic signal shapes that deviate in some way from the Gaussian form were observed. Five characteristic shapes were identified and classified. The five shapes shown in Fig. 4, which are optically-scanned photographs of actual oscilloscope traces, are described as follows: (a) characterized by a Gaussian distribution; (b) characterized by an asymmetric distribution about the maximum amplitude due to a slow decay of the decreasing portion of the signal; (c) characterized by the apparent superposition of two droplet traces slightly out of phase; (d) characterized by a symmetric distribution about the maximum amplitude point with gradually increasing

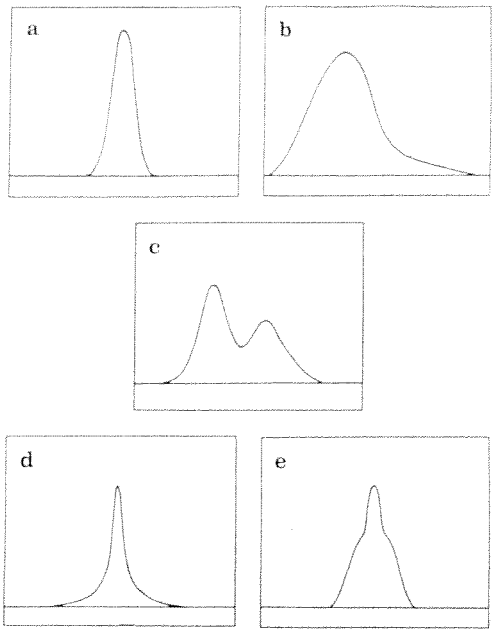

Fig. 4a–e. Droplet type signatures

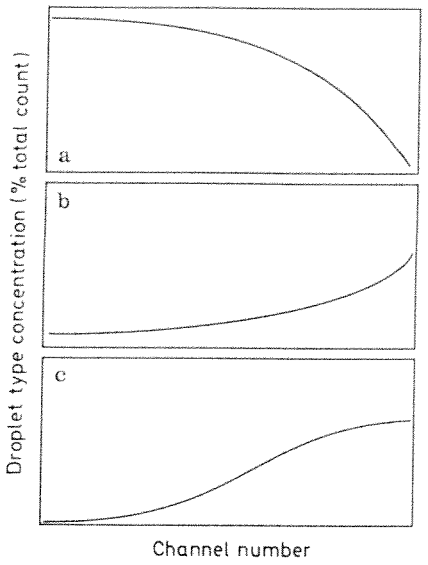

Fig. 5a–c. Droplet type concentrations

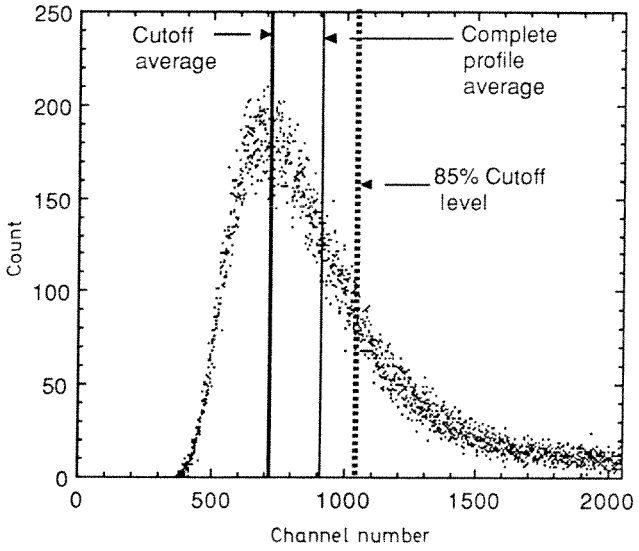

Fig. 6. Typical raw data (TAC signals) distribution

slope from the base to the peak; (e) characterized by a symmetrical distribution about the maximum amplitude point with two distinct slopes, a low slope far from the peak and a high slope near the peak.

Although the cause for each of these signatures is left to future work, some assessment of the characteristics can be made. Experimental observations have determined that types (a), (b) and (c) occupy the vast majority ($\sim 95\%$) of the number concentration. Therefore, types (d) and (e) are not considered further. As linear operator theory predicts, a Gaussian droplet signature, type (a), which best approximates this form, is assumed to be a spherical droplet. Type (b) is postulated to be an asymmetric droplet with an aspect ratio greater than 2 : 1, and type (c) is assumed to result from two droplets in the measurement volume at approximately the same time. These assumptions form the basis of the cutoff voltages and lead to the statement that the cutoff average represents a theoretically valid speed measurement.

Due to the difficulty of measuring the speed of a ligament or "droplet" with aspect ratios greater than 2 : 1, it is appropriate to restrict the analysis to the speed measurement of those droplets with aspect ratios less than 2 : 1. Additional analysis of the droplet number concentrations leads to the qualitative representation shown in Fig. 5. This figure presents the droplet type normalized concentration, catalogued as described previously versus MCA channel number, i.e., voltage, which is inversely proportional to speed. The distribution forms shown in this figure are representative of all data sets examined. Note that the actual data does not exhibit this monotonic behavior precisely. These qualitative droplet concentrations lead to the assumption that a discrimination level can be established to restrict the analysis to the desired droplet type. An absolute cutoff or discrimination level does not exist due to the convolution of the three droplet types as shown in the figure. Hence, for the present experiment, an arbitrary voltage level, below which at least 85% of the events depict droplets of type (a), defines the cutoff level.

Fig. 6 shows the effect of the cutoff voltage level on a typical MCA distribution. Recall that the channel number relates directly to the voltage and inversely to the speed. Therefore, the effect of the cutoff voltage is to increase the droplet speed, as seen in Fig. 3. The cutoff level is an arbitrarily chosen experimental value which varies with applied voltage and measurement station, as listed in Table 1. As a result of the arbitrary nature of this choice, its effect on the error in the speed measurement is not considered.

Table 1. Experimental cutoff voltage levels

Axial position [cm]	Applied voltage [kV]	Cutoff voltage [V]
1.3 ± 0.1	15.0	4.70
	17.5	4.67
	20.0	4.30
	22.5	4.67
	25.0	4.40
	27.5	4.20
3.0 ± 0.1	15.0	8.00
	20.0	7.75
	25.0	5.75

The data presented in Table 1 shows a general decrease in cutoff voltage, corresponding to an increase in the minimum Gaussian subpopulation speed, with increasing applied voltage. This effectively means that the Gaussian subpopulation follows the general trends of the spray seen in Fig. 3. The data shows a more pronounced rate of change in cutoff voltage with applied voltage at the 3.0 cm station than at the 1.3 cm station. The rate of change in average speeds, however, remains essentially constant over the experimental range (see Fig. 3). Investigating the discrepancies in these rates and considering their effect on the MCA profile curves (see Fig. 6), leads to the conclusion that a greater number of droplet events occur at the lower MCA voltages with increasing applied voltage. This increase in events is greater than that due to the speed increase with applied voltage alone. Because the majority of these events below the cutoff voltage level are postulated to be type (a), the relative concentration of type (a) is, therefore, assumed to be increasing with applied voltage. This assumption follows the general trends of the EHD spray in which the droplet size decreases with applied voltage (Snarski 1988). As the size of the droplet decreases, so does the relaxation time for the droplet to fully collapse from the ligament to the spherical droplet. Therefore, the relative concentration of spherical droplets increases with increasing applied voltage, which, in turn, effectively shortens the developing region. The data in Table 1 also shows that at the 3.0 cm station, the magnitude of the cutoff voltages are significantly higher than at the 1.3 cm station. This effect results from the decrease in droplet speed with increasing axial station. Note also that the effect of the cutoff voltage method on the speed determination diminishes with increasing axial station (Fig. 3). This results from the fact that an increase in the axial measurement station approaches the extent of the developing region where the cutoff voltage method becomes redundant.

In this experiment, speed measurements for the non-Gaussian subpopulations are not investigated. These subpopulations are only noted, defined, and qualitatively discussed in terms of possible generation methods. Speed errors associated with their inclusion in the Gaussian subpopulation treat them as a whole. Recall that the speeds used to assess the PCSV-E ability in the developing region result from method (3). The speeds determined by methods (1) and (2) are presented only for comparison purposes.

4.2 Experimental errors

After investigating the cutoff voltages correlations with droplet speed (and size) variation and their effects on the speed measurement, the errors associated with the operation of the PCSV-E system per se can be assessed. The PCSV-E technique measures a transit time by the combined circuitry of the PSA and the TAC. The speed is then determined by the simple equation in which speed = distance/time, where distance is an analytical result of the Gaussian intensity distribution of the measurement volume (TTD). The component of the speed error in this expression can be found by considering the uncertainties in the distance and time. Because these uncertainties are independent and assumed random (an assumption invoked for all measured quantities), the uncertainty in the speed follows from the general formula for error propagation (Taylor 1982). The uncertainty in the time results from a combination of the individual uncertainties of each component in the timing sequence from PSA through to the Macintosh II. This sequence yields an uncertainty of less than 0.3% (Grace 1990). An uncertainty in the distance exists because of the lack of agreement between semi-independent methods of speed measurement in the calibration procedure. This lack of agreement dictates a choice between two fundamental experimental constants, the laser beam diameter at the focal point or the reticle radius. Allowing both constants to retain their reference values generates incompatible calibration speeds. Either constant can be specified because no acceptable comparison standard exists.

In this experiment, the referenced reticle radius value is used.[1] This then dictates a corrected beam diameter, or equivalently a TTD, such that the calibration speeds agree within error. The effect of this choice is apparent in Fig. 3 where a 10% speed difference between methods (1) and (2) results from the particular TTD used, either the referenced or the calibrated value. The uncertainty resulting from the calibration work in the TTD is ±1.8%. The final uncertainty associated with the speed equation, by the error propagation formula, is ±1.8%. Note that this is an error associated with the speed equation itself and not the measurements. Hence, the PCSV-E can perform no better than this value.

The experimental component of the error associated with the application of the PCSV-E to the developing region of the EHD spray involves the selection of the PSA lower discriminator level. The selection of the TAC discriminator does not involve an error by virtue of its overlap capability. Selection of the PSA lower discriminator level can affect the final speed determination as seen in Fig. 7. This figure shows a representative variation in speed with PSA lower discrim-

[1] Independent measurement of the reticle radius using a metalograph have recently verified the radius to within 2% of the reference value

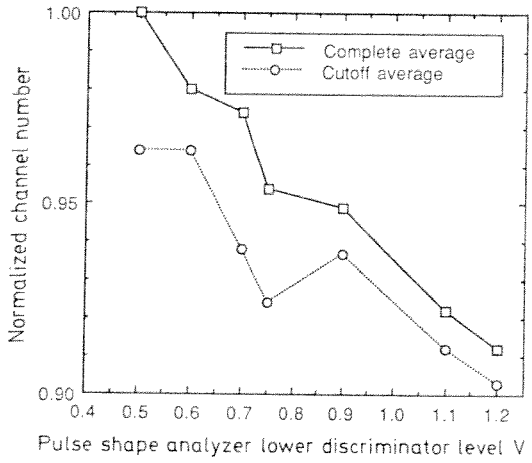

Fig. 7. PSA lower discriminator level effect on speed measurement

inator level selection. Note that this figure uses a normalized channel number to represent a nondimensional speed for the parameter set. The limits in this figure are experimentally imposed. Above 1.2 V, the data rate falls to an unacceptably low level, indicating a significant bias of the results. Below the minimum level, the data rate increases to an unacceptably high level, indicating invalid trajectories, i.e., droplets sweeping the edge of the measurement volume or outside the theoretically valid area. The lack of monotonic variation and the desire to express the uncertainty associated with the PSA lower discriminator level for all experimental parameters by the same method, results in an uncertainty calculated by the maximum speed deviation for a parameter set (see Fig. 7) divided by the speed result for that particular parameter set.

The final assessment of the PCSV-E capability in the developing region of the spray results from the combination of the experimental uncertainty (PSA lower discriminator level) with the uncertainty in the speed equation by the above method of error propagation. The resultant errors vary with voltage and measurement station due to the nature of the EHD spray and the effect of the characteristic time scale relevant to the developing region. Droplet characteristics exhibit small differences with applied voltage within the broader definition of the fine spray mode. These differences do not indentically affect the PCSV-E system. The definition of the developing region implicitly assumes a time dependence or, equivalently, a dependence on axial measurement station of droplet characteristics. This dependence will in turn affect the performance of the PCSV-E provisorily. The results of this particular experiment determine that the PCSV-E has the ability to measure droplet speed in the developing region of the fine spray mode of the subject EHD spray with an average uncertainty of 3.0% and a corresponding maximum uncertainty of 6.0%.

5 Conclusions

Experiments conducted to assess the ability of the PCSV-E technique to measure droplet speeds in the developing region of the fine spray mode of the EHD spray have shown that the technique performs well in a region not generally accessible to laser diagnostics. The results indicate that the PCSV-E can resolve droplet speeds with an average uncertainty of 3.0% and with a maximum uncertainty of less than 6.0%. The speed reduction method used in this paper determines a cutoff voltage which discriminates out a given percentage of defined invalid signals such that the resulting speed is theoretically valid. This method relies on the ability of the PCSV-E to resolve droplets with aspect ratios of up to 2 : 1. This cutoff method preserves the trends of an EHD spray as seen by other investigators. The PCSV-E technique has been applied to other types of aerosol with similar success (Holve 1982) and offers an excellent method for measuring droplet parameters in a developing region permeated by complex geometries.

References

Abernathy, R. B.; Benedict, R. P.; Dowdell, R. B. 1985: ASME measurement uncertainty. J. Fluids Eng. 107, 161–164

Bailey, A. G. 1988: Electrostatic spraying of liquids. New York: Wiley

Drozin, V. G. 1954: The electrical dispersion of liquids as aerosols. Dept. of Chem., Columbia University, 158–164

Dunn, P. F.; Snarski, S. R. 1991: Droplet diameter, flux and total current measurements in an electrohydrodynamic spray. Phys. Fluids A. 3, 492–494

Gomez, A.; Tang, K. 1990: Characterization of liquid fuel electrostatic sprays. Paper presented at the Western States Section/Comb. Inst. 1990 Fall Meeting

Grace, J. M. 1990: Droplet speed measurements in the developing region of an electrohydrodynamic spray using laser diagnostics. M.S. Thesis, University of Notre Dame: Notre Dame

Hayati, I.; Bailey, A.; Tadros, Th. F. 1987: Investigations into the mechanism of electrohydrodynamic spraying of liquids, Part I and Part II. J. Colloid Interface Sci. 117, 205–230

Hirleman, D. E. 1978: Laser technique for simultaneous particle-size and velocity measurements. Opt. Lett. 3, 19–21

Hirleman, D. E.; Stevenson, W. H. 1978: Intensity distribution properties of a Gaussian laser beam focus. App. Opt. 17, 3496–3499

Holve, D. J. 1982: Transit timing velocimetry (TTV) for two-phase reacting flows. Comb. Flame. 48, 105–108

Holve, D. J.; Annen, K. D. 1984: Optical particle counting, sizing, velocimetry using intensity deconvolution integral. Opt. Eng. 23, 592–602

Holve, D.; Self, S. 1979: Optical particle sizing for in situ measurements, Part 1. App. Opt. 18, 1632–1645

Innes, D. J.; Bloom, A. L. 1966: Design of optical systems for use with laser beams. Spectra-Physics Laser Tech. Bull. 5, 1–10

Insitec 1990: Manual for PCSV. San Ramon, CA: Insitec

Kline, S. J. 1985: The purpose of uncertainty analysis. J. Fluids Eng. 107, 153–160

Snarski, S. R. 1988: The interaction of electrohydrodynamically generated liquid droplets. M.S. Thesis, Univ. of Notre Dame: Notre Dame

Taylor, J. R. 1982: An introduction to error analysis. Mill Valley, CA: Oxford University Press

Wilson, J.; Hawkes, J. F. B. 1987: Lasers: principles and applications. United Kingdom: Prentice Hall

Received June 26, 1991